Dipole polarizabilities of light pseudoscalar mesons within the domain model of the QCD vacuum

Sergei Nedelko[*] and Vladimir Voronin[†]

Joint Institute for Nuclear Research, 141980 Dubna, Moscow Region, Russia

(Received 24 August 2022; accepted 3 May 2023; published 22 May 2023)

Dipole polarizabilities of light pseudoscalar mesons are calculated in the framework of the mean field approach to QCD vacuum and bosonization based on the statistical ensemble of almost everywhere homogeneous Abelian (anti-)self-dual gluon fields, the domain model of QCD vacuum. In this approach, a nonlocal effective action of meson fields is derived that describes all possible strong, weak, and electromagnetic interactions of meson fields including their excited states. The considered mean field implements confinement and chiral symmetry, which manifests itself both in the properties of quark and gluon fields as well as upon bosonization, in the mass spectrum, decays constants and form factors of nonlocal colorless hadrons, and leads to the qualitatively distinctive features of the effective meson action. Particularly relevant to the subject of the present paper are the nonlocality of meson-quark-antiquark vertices and the absence of poles at real momenta in the propagators of scalar meson fields composed of light quark-antiquark pairs. In view of this, studying the role of manifest nonlocality of mesons and contribution of intermediate scalar meson fields in formation of the polarizabilities is of special interest. It turns out that, for charged pions and kaons, this contribution is substantial but not the largest one. Nonlocal nature of mesons provides an additional contribution so that calculated polarizabilities are in reasonable agreement with COMPASS experimental data and chiral perturbation theory.

DOI: 10.1103/PhysRevD.107.094027

I. INTRODUCTION

Polarizabilities of hadrons characterize their response to an applied electromagnetic field, which cannot be attributed to pointlike particles and are of fundamental interest for low-energy QCD. Experimental measurement of polarizabilities is challenging, so most data are available for lightest mesons $\pi^{\pm}$, π^0, but there is a long-standing discrepancy in the values (see papers [1–3] for a review of the theoretical and experimental status of the meson polarizability problem). Among the reported experimental results, only the most recent data on charged pion polarizability by COMPASS collaboration at CERN [4] is consistent with chiral perturbation theory (ChPT). The leading-order result of ChPT [5] is equivalent to the value found in Ref. [6] based on the hypothesis of partially conserved axial-vector current.

The polarizabilities were investigated theoretically within chiral perturbation theory up to two loops [7–11], with the methods of lattice QCD [12–22], within various phenomenological models [23–30], and with the help of dispersion relations [31–33]. Several studies [27,28,30,32] found that the dominating part of pion polarizabilities is due to the σ meson. In the present study, polarizabilities are extracted from the nonlocal effective meson action deduced within the domain model of the QCD vacuum and hadronization (see Refs. [34–38]).

In this action meson fields appear as collective colorless excitations of confined dynamical quark-antiquark, heavy and light ones, and gluon fields. A highly nonlocal effective meson action contains information about the strong, weak, and electromagnetic interactions of mesons as well as their two-point correlation functions. In particular, the model systematically describes various phenomena related to confinement and chiral symmetry realization, the heavy quark limit. Meson masses, including the Regge spectrum of excited states of mesons, their decay constants, and form factors are in good agreement with experimental values [34–40].

The specific feature of this approach is that mesons appear as extended composite fields due to nonlocal meson-quark vertices. Meson masses are identified as

[*]nedelko@theor.jinr.ru
[†]voronin@theor.jinr.ru

the poles of the nonlocal meson propagators. As it turns out, there are no poles at real momenta in the nonlocal propagators of the scalar mesonlike composite fields, and therefore light scalar mesons as quark-antiquark states are absent in the physical spectrum of the stable collective excitations. This property relates to the peculiarities of realization of chiral symmetry in the presence of an Abelian (anti-)self-dual gluon mean field and agrees with expectation that the lightest scalar state σ is not intuitively made of a quark and an antiquark [41]. At the same time, scalar mesonlike fields contribute to the amplitudes of various processes. It has to be noted that physical scalar states occur in the hyperfine splitting of the orbital excitations of the vector mesons with the masses above 1 GeV.

We describe the formalism and its features in Sec. II. In Sec. III we calculate polarizabilities and find that charged pion polarizability is consistent with ChPT [7] and COMPASS data [4]. The contribution of intermediate scalar meson fields to polarizability of pion and kaon is substantial, especially for the neutral ones, while for charged pion and kaon polarizability the intermediate scalar meson turns out to be less important.

II. EFFECTIVE MESON ACTION

The mean-field approach based on the random Abelian (anti-)self-dual vacuum gluon fields allows us to deduce a generating functional via bosonization of one-gluon exchange interaction of quark currents, which has the form [34–39]

$$Z = \mathcal{N}\int D\phi_{\mathcal{Q}}\exp\Big\{-\frac{\Lambda^2}{2}\frac{h_{\mathcal{Q}}^2}{g^2C_{\mathcal{Q}}^2}\int d^4x\phi_{\mathcal{Q}}^2(x) - \sum_{k=2}^{\infty}\frac{1}{k}W_k[\phi]\Big\}, \tag{1}$$

$$W_k[\phi] = \sum_{\mathcal{Q}_1\ldots\mathcal{Q}_k} h_{\mathcal{Q}_1}\ldots h_{\mathcal{Q}_k}\int d^4x_1\ldots\int d^4x_k\Phi_{\mathcal{Q}_1}(x_1)\ldots \times\Phi_{\mathcal{Q}_k}(x_k)\Gamma^{(k)}_{\mathcal{Q}_1\ldots\mathcal{Q}_k}(x_1,\ldots,x_k), \tag{2}$$

$$\Phi_{\mathcal{Q}}(x) = \int\frac{d^4p}{(2\pi)^4}e^{ipx}\mathcal{O}_{\mathcal{Q}\mathcal{Q}'}(p)\tilde{\phi}_{\mathcal{Q}'}(p), \qquad C_{\mathcal{Q}} = C_J, \qquad C^2_{S/P} = 2C^2_{V/A} = \frac{1}{9}. \tag{3}$$

The condensed index $\mathcal{Q}\equiv\{aJLn\}$ includes all quantum numbers of a meson, Λ is a scale related to the strength of the vacuum gluon field, and finally to the value of gluon condensate $\langle g^2F^2\rangle$. The physical color neutral meson fields $\phi_{\mathcal{Q}}$ are obtained by means of orthogonal transformation $\mathcal{O}_{\mathcal{Q}\mathcal{Q}'}$ of fields $\Phi_{\mathcal{Q}}$. The quadratic part of the action for $\phi_{\mathcal{Q}}$ is diagonal with respect to all quantum numbers. The masses of mesons correspond to the poles of nonlocal propagators

$$D_{\mathcal{Q}}(p^2) = h_{\mathcal{Q}}^{-2}\left(\frac{\Lambda^2}{g^2C_{\mathcal{Q}}^2}+\tilde{\Gamma}^{(2)}_{\mathcal{Q}}(p^2)\right)^{-1} \tag{4}$$

and can be found as zeroes of the inverse propagator from the equation

$$0 = \frac{\Lambda^2}{g^2C_{\mathcal{Q}}^2}+\tilde{\Gamma}^{(2)}_{\mathcal{Q}}(-M^2_{\mathcal{Q}}), \tag{5}$$

where $\tilde{\Gamma}^{(2)}_{\mathcal{Q}}$ is two-point correlation function diagonalized with respect to all quantum numbers. Constants $h_{\mathcal{Q}}$ are defined by the equation

$$1 = h^2_{\mathcal{Q}}\frac{d}{dp^2}\tilde{\Gamma}^{(2)}_{\mathcal{Q}}(p^2)\Big|_{p^2=-M^2_{\mathcal{Q}}},$$

which ensures that the residue at the pole of the propagator is equal to unity. The results of calculation of the masses of various mesons as well as analytical expressions of $\tilde{\Gamma}^{(2)}_{\mathcal{Q}}(p^2)$ can be found in Ref. [35]. In the one-loop approximation, the meson propagators given by Eq. (4) are real, and therefore mesons are stable with respect to decay into quarks by virtue of the optical theorem. It is also quite plausible that correlation functions of a greater number of external mesons are suppressed as the number of colors N_c approaches infinity because the functional (1) is deduced from QCD. A thorough investigation of this limit is an interesting topic to be studied in the future.

Correlation functions include "connected" and "disconnected" contributions of quark loops in the background field. For example, the two-point nonlocal vertex function $\tilde{\Gamma}^{(2)}_{\mathcal{Q}\mathcal{Q}'}(p)$ is given by

$$\Gamma^{(2)}_{\mathcal{Q}_1\mathcal{Q}_2} = \overline{G^{(2)}_{\mathcal{Q}_1\mathcal{Q}_2}(x_1,x_2)} - \Xi_2(x_1-x_2)\overline{G^{(1)}_{\mathcal{Q}_1}G^{(1)}_{\mathcal{Q}_2}}, \tag{6}$$

where Ξ is correlation function of the background field that belongs to the statistical ensemble of the almost everywhere homogeneous Abelian (anti-)self-dual fields. Quark loops $G^{(k)}_{\mathcal{Q}_1\ldots\mathcal{Q}_k}$ are averaged over the ensemble of background field configurations with the measure $d\sigma_B$:

$$\overline{G^{(k)}_{\mathcal{Q}_1\ldots\mathcal{Q}_k}(x_1,\ldots,x_k)} = \int d\sigma_B \mathrm{Tr} V_{\mathcal{Q}_1}(x_1) S(x_1,x_2)\ldots V_{\mathcal{Q}_k}(x_k) S(x_k,x_1), \overline{G^{(l)}_{\mathcal{Q}_1\ldots\mathcal{Q}_l}(x_1,\ldots,x_l) G^{(k)}_{\mathcal{Q}_{l+1}\ldots\mathcal{Q}_k}(x_{l+1},\ldots,x_k)}$$
$$= \int d\sigma_B \mathrm{Tr}\{V_{\mathcal{Q}_1}(x_1) S(x_1,x_2)\ldots V_{\mathcal{Q}_k}(x_l) S(x_l,x_1)\}\mathrm{Tr}\{V_{\mathcal{Q}_{l+1}}(x_{l+1}) S(x_{l+1},x_{l+2})\ldots V_{\mathcal{Q}_k}(x_k) S(x_k,x_{l+1})\}. \tag{7}$$

Here $S(x,y)$ is the quark propagator and $V_{\mathcal{Q}}$ are nonlocal meson-quark-antiquark vertices.

The quark propagator and meson-quark vertices in the presence of the almost everywhere homogeneous fields are approximated by those in the homogeneous (anti-)self-dual Abelian background field. The averaging over mean field ensemble is achieved by averaging the quark loops over configurations of the homogeneous background fields, supplemented by taking into account n-point correlators of the mean fields Ξ_n. The averaging is performed over self-dual and anti-self-dual Abelian (anti-)self-dual configurations and their directions in Euclidean and color spaces. Averaging over spatial directions in R^4 is performed with the help of generating formula

$$\int d\sigma_B \exp(i f_{\mu\nu} J_{\mu\nu}) = \langle \exp(i f_{\mu\nu} J_{\mu\nu})\rangle = \frac{\sin\sqrt{2(J_{\mu\nu}J_{\mu\nu} \pm J_{\mu\nu}\tilde{J}_{\mu\nu})}}{\sqrt{2(J_{\mu\nu}J_{\mu\nu} \pm J_{\mu\nu}\tilde{J}_{\mu\nu})}}, \tag{8}$$

where $J_{\mu\nu}$ is an arbitrary antisymmetric tensor. Tensor $f_{\mu\nu}$ is an appropriately normalized Abelian (anti-)self-dual background field with strength Λ:

$$\hat{B}_\mu = -\frac{1}{2}\hat{n} B_{\mu\nu} x_\nu, \qquad \hat{n} = t^3\cos\xi + t^8 \sin\xi,$$
$$\tilde{B}_{\mu\nu} = \frac{1}{2}\epsilon_{\mu\nu\alpha\beta} B_{\alpha\beta} = \pm B_{\mu\nu}, \qquad \hat{B}_{\rho\mu}\hat{B}_{\rho\nu} = 4\upsilon^2\Lambda^4\delta_{\mu\nu},$$
$$f_{\alpha\beta} = \frac{\hat{n}}{2\upsilon\Lambda^2} B_{\alpha\beta}, \qquad \upsilon = \mathrm{diag}\left(\frac{1}{6},\frac{1}{6},\frac{1}{3}\right), \qquad f_{\mu\alpha} f_{\nu\alpha} = \delta_{\mu\nu}, \tag{9}$$

where the upper sign in "±" should be taken for a self-dual field, and the lower for an anti-self-dual field. Nonlocal vertices $V^{aJln}_{\mu_1\ldots\mu_l}$ are given by the following formulas:

$$V^{aJln}_{\mu_1\ldots\mu_l} = \mathcal{C}_{ln}\mathcal{M}^a\Gamma^J F_{nl}\left(\frac{\overleftrightarrow{\mathcal{D}}^2(x)}{\Lambda^2}\right) T^{(l)}_{\mu_1\ldots\mu_l}\left(\frac{1}{i}\frac{\overleftrightarrow{\mathcal{D}}(x)}{\Lambda}\right),$$
$$\mathcal{C}^2_{ln} = \frac{l+1}{2^l n!(n+l)!}, \qquad F_{nl}(s) = s^n\int_0^1 dt t^{n+l}\exp(st),$$
$$\overleftrightarrow{\mathcal{D}}^{ff'}_\mu = \xi_f\overleftarrow{\mathcal{D}}_\mu - \xi_{f'}\overrightarrow{\mathcal{D}}_\mu, \qquad \overleftarrow{\mathcal{D}}_\mu(x) = \overleftarrow{\partial}_\mu + i\hat{B}_\mu(x), \qquad \overrightarrow{\mathcal{D}}_\mu(x) = \overrightarrow{\partial}_\mu - i\hat{B}_\mu(x),$$
$$\xi_f = \frac{m_{f'}}{m_f + m_{f'}}, \qquad \xi_{f'} = \frac{m_f}{m_f + m_{f'}}. \tag{10}$$

Here $\mathcal{M}^a$ and Γ^J are flavor and Dirac matrices corresponding to a given meson field, constantsξ_f, $\xi_{f'}$ ensure that x is the center of mass of a meson and n, l are radial and orbital quantum numbers, respectively. Radial part F_{nl} is defined by the propagator of the gluon fluctuations charged with respect to the Abelian background and $T^{(l)}$ are irreducible tensors of four-dimensional rotation group. Propagator of the quark with mass m_f in the presence of the homogeneous Abelian (anti-)self-dual field has the form

$$S_f(x,y) = \exp\left(-\frac{i}{2}\hat{n} x_\mu B_{\mu\nu} y_\nu\right) H_f(x-y),$$
$$\tilde{H}_f(p) = \frac{1}{2\upsilon\Lambda^2}\int_0^1 ds e^{(-p^2/2\upsilon\Lambda^2)s}\left(\frac{1-s}{1+s}\right)^{m_f^2/4\upsilon\Lambda^2}\left[p_\alpha\gamma_\alpha \pm i s\gamma_5\gamma_\alpha f_{\alpha\beta}p_\beta + m_f\left(P_\pm + P_\mp\frac{1+s^2}{1-s^2} - \frac{i}{2}\gamma_\alpha f_{\alpha\beta}\gamma_\beta\frac{s}{1-s^2}\right)\right], \tag{11}$$

where the anti-Hermitean representation of Dirac matrices is used, and the "±" signs are arranged in accordance with formula (9). The translation-invariant part H_f of the propagator is an analytical function in the finite complex momentum plane and matches the behavior of free Dirac propagator at large Euclidean momentum. The analyticity of the quark propagator is interpreted as the confinement of dynamical quarks.

Overall, the mass spectrum of the ground state and excited mesons composed of light and heavy quarks is described rather accurately, in complete agreement with expectations based on confinement (Regge mass spectrum of radially and orbitally excited states) and chiral symmetry breaking (light pseudoscalar and heavy vector nonets, etc.) as well as asymptotic heavy-quark relations.

A peculiar property of the quark propagator in the mean gluon field under consideration is that, unlike the case of the pseudoscalar and vector ground-state mesons, there are no real solutions to Eq. (5) for their parity partners, the ground-state scalar and axial mesons. Axial and scalar mesons appear with a mass above 1 GeV in the hyperfine splitting of the orbital excitations. The inverse propagators of pseudoscalar and scalar meson fields are shown in Fig. 1, which manifestly illustrates the absence of a pole for the scalar field propagator. This feature is particularly relevant to the present study. Contributions of intermediate scalar mesonlike fields to various processes are available and can be computed but a controversial issue of existence of the light scalar mesons does not occur.

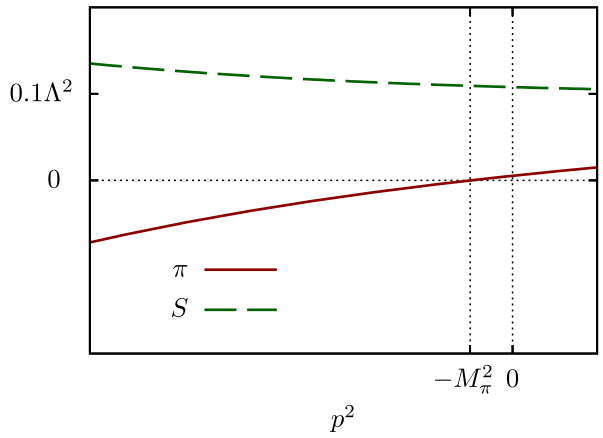

FIG. 1. Left-hand side of Eq. (5) (which is proportional to the inverse propagator) for pion and ground-state scalar quark-antiquark field with respect to Euclidean momenta p^2. The zero of inverse pion propagator [correspondingly, the pole of propagator $D_\pi(p^2)$] is located at $-M_\pi^2$, while inverse propagator $D_S^{-1}(p^2)$ has no zeroes at real momenta.

Though the meson-quark coupling constant $h_\mathcal{Q}$ is obviously undefined for mesonlike composite fields if the corresponding Eq. (5) has no solutions, it is convenient to retain it in order to have universal notation. Such fields can only be virtual, and $h_\mathcal{Q}$ cancels out in the final expressions ($h_\mathcal{Q}^2$ for two vertices cancel $h_\mathcal{Q}^{-2}$ in propagator $D_\mathcal{Q}$).

Electromagnetic interactions are included in gauge-invariant way using the prescription of Ref. [42], which yields expansions (see Refs. [35,43])

$$S_f(x,y|A) = S_f(x,y) + \sum_{n=1}^{\infty} (Q_f e)^n \int dz_1 \cdots \int dz_n S_f(x_1,z_1)\gamma_{\mu_1} A_{\mu_1}(z_1) \cdots S_f(z_{i-1},z_i)\gamma_{\mu_i} A_{\mu_i}(z_i) \cdots S_f(z_n,y),$$

$$V_\mathcal{Q}(x|A) = V_\mathcal{Q}(x) + \sum_{n=1}^{\infty} e^n \int dz_1 \cdots \int dz_n V_{\mathcal{Q}\mu_1\ldots\mu_n}(x,z_1,\ldots,z_n) A_{\mu_1}(z_1) \cdots A_{\mu_n}(z_n),$$

where Q is a diagonal matrix of quark charges in units of electron charge e, and meson-photon vertices appear due to nonlocality of meson-quark interactions. One-photon and two-photon meson vertices are given by

$$V_{\mathcal{Q}\mu}(x;q) = \int_0^1 d\tau \frac{1}{\tau} \frac{\partial}{\partial q_\mu} \{-Q_f V_\mathcal{Q}(\overleftrightarrow{\mathcal{D}}(x) - iq\tau\xi) + Q_{f'} V_\mathcal{Q}(\overleftrightarrow{\mathcal{D}}(x) + iq\tau\xi')\}, \tag{12}$$

$$\begin{aligned} V_{\mathcal{Q}\mu\nu}(x;q_1,q_2) = \frac{1}{2}\int_0^1 d\tau_1 \int_0^1 d\tau_2 \frac{1}{\tau_1\tau_2} \frac{\partial}{\partial q_{1\mu}} \frac{\partial}{\partial q_{2\nu}} [&Q_f Q_{f'} V_\mathcal{Q}(\overleftrightarrow{\mathcal{D}}(x) - iq_1\tau_1\xi - iq_2\tau_2\xi) \\ &- Q_f Q_{f'} V_\mathcal{Q}(\overleftrightarrow{\mathcal{D}}(x) - iq_1\tau_1\xi + iq_2\tau_2\xi) - Q_{f'} Q_f V_\mathcal{Q}(\overleftrightarrow{\mathcal{D}}(x) + iq_1\tau_1\xi - iq_2\tau_2\xi) \\ &+ Q_{f'} Q_{f'} V_\mathcal{Q}(\overleftrightarrow{\mathcal{D}}(x) + iq_1\tau_1\xi + iq_2\tau_2\xi)], \end{aligned} \tag{13}$$

where Q_f is the electric charge of a quark with flavor f.

The generating functional and the effective meson action take the form

$$Z = \mathcal{N}\int D\phi_{\mathcal{Q}}\int DA_\mu \exp\left\{-\frac{1}{4}\int d^4x F_{\mu\nu}F_{\mu\nu} - \frac{\Lambda^2}{2}\frac{h_{\mathcal{Q}}^2}{g^2C_{\mathcal{Q}}^2}\int d^4x\phi_{\mathcal{Q}}^2(x) - \Gamma(A) - \sum_{k=2}^{\infty}\frac{1}{k}W_k[\phi|A]\right\},$$
$$W_k[\phi|A] = \sum_{\mathcal{Q}_1\ldots\mathcal{Q}_k} h_{\mathcal{Q}_1}\ldots h_{\mathcal{Q}_k}\int d^4x_1\ldots\int d^4x_k\Phi_{\mathcal{Q}_1}(x_1)\ldots\Phi_{\mathcal{Q}_k}(x_k)\Gamma^{(k)}_{\mathcal{Q}_1\ldots\mathcal{Q}_k}(x_1,\ldots,x_k|A), \tag{14}$$

where

$$\Gamma(A) = \int d\sigma_B \mathrm{Tr}\log\left[1 + Qe\gamma_\mu A_\mu(x)S(x,y)\right]$$

and $\Gamma^{(k)}_{\mathcal{Q}_1\ldots\mathcal{Q}_k}(x_1,\ldots,x_k|A)$ are obtained from $\Gamma^{(k)}_{\mathcal{Q}_1\ldots\mathcal{Q}_k}(x_1,\ldots,x_k)$ by substitutions

$$S_f(x,y) \to S_f(x,y|A), \qquad V_{\mathcal{Q}}(x) \to V_{\mathcal{Q}}(x|A).$$

The free parameters of the model are scale Λ (scalar gluon condensate), infrared limits of dynamical quark masses and strong coupling α_s, which has been determined by fitting to the masses of mesons π, ρ, K, K^*, J/ψ, Υ, η' (for details see Ref. [35]).

As it has been mentioned, the diagonalization of the quadratic part of the effective action (2) with respect to the radial quantum number is a part of the calculation procedure. In practice some finite number of excited states can be taken into account. As it has been analyzed in [35], though typically about five lowest radial states have to be taken into account for robust stability of the computation, a consistent overall description of the mass spectrum of mesons is achieved irrespective to a number of accounted radial excitations. Just the values of the free parameters have to be adjusted when the number of accounted radial excitation changes.

III. EVALUATION OF POLARIZABILITIES

The polarizabilities are defined by the Compton scattering amplitude

$$P(p) + \gamma(q,\varepsilon) \to P(p') + \gamma(q',\varepsilon')$$

of a pseudoscalar meson P

$$_{\mathrm{out}}\langle P(p')\gamma(q',\varepsilon')|P(p)\gamma(q,\varepsilon)\rangle_{\mathrm{in}} = i(2\pi)^4\delta^{(4)}(p'+q'-p-q)\varepsilon^\mu(q)\varepsilon^{*\nu}(q')M_{\mu\nu}.$$

We concentrate on the electric α_{E} and magnetic β_{M} dipole polarizabilities that appear in expansion of the amplitude in small photon momenta as

$$\varepsilon^\mu(q)\varepsilon^{*\nu}(q')M_{\mu\nu} = -2e^2\vec{\varepsilon}\cdot\vec{\varepsilon}'^* + 8\pi M(\alpha_{\mathrm{E}}\omega\omega'\vec{\varepsilon}\cdot\vec{\varepsilon}'^* + \beta_{\mathrm{M}}(\vec{\varepsilon}\times\vec{q})\cdot(\vec{\varepsilon}'^*\times\vec{q}')) + \ldots,$$

where M is the mass of a pseudoscalar meson. The tensor $M_{\mu\nu}$ can be separated into two parts

$$M_{\mu\nu} = M^{\mathrm{Born}}_{\mu\nu} + M^{\mathrm{NB}}_{\mu\nu}, \tag{15}$$

where the part $M^{\mathrm{NB}}_{\mu\nu}$ describes the response of a meson as a composite system to the applied electromagnetic field. The term $M^{\mathrm{Born}}_{\mu\nu}$ given by

$$M^{\mathrm{Born}}_{\mu\nu} = e^2\left[2g_{\mu\nu} - \frac{(2p_\mu+q_\mu)(2p'_\nu+q'_\nu)}{(p+q)^2-M^2} - \frac{(2p_\nu-q'_\nu)(2p'_\mu-q_\mu)}{(p-q')^2-M^2}\right] \tag{16}$$

describes real Compton scattering of a structureless pseudoscalar particle.

In the case of real Compton scattering ($q^2 = q'^2 = 0$, $\varepsilon^\mu(q)q_\mu = \varepsilon^{*\mu}(q')q'_\mu = 0$), the tensor $\mathcal{M}_{\mu\nu}$ contains only two independent tensor structures [44–46]

$$\varepsilon^\alpha(q)\varepsilon^{*\beta}(q')M_{\alpha\beta} = \varepsilon^\alpha(q)\varepsilon^{*\beta}(q')(AT_{1\alpha\beta} + BT_{2\alpha\beta}),$$
$$T_{1\alpha\beta} = -\frac{t}{2}g_{\alpha\beta} - q_\beta q'_\alpha,$$
$$T_{2\alpha\beta} = -\frac{t}{2}P_\alpha P_\beta + \nu^2 g_{\alpha\beta} - \nu(P_\alpha q_\beta + P_\beta q'_\alpha), \tag{17}$$

where

$$P = \frac{p+p'}{2}, \qquad s = (p+q)^2, \qquad t = (q-q')^2,$$
$$u = (p-q')^2, \qquad \nu = \frac{1}{4}(s-u).$$

In accordance with Eqs. (15) and (16), amplitudes A and B can be split in two parts

$$A(\nu^2,t) = A^{\mathrm{Born}}(\nu^2,t) + A^{\mathrm{NB}}(\nu^2,t),$$
$$B(\nu^2,t) = B^{\mathrm{Born}}(\nu^2,t) + B^{\mathrm{NB}}(\nu^2,t),$$

where A^{Born}, B^{Born} are given by

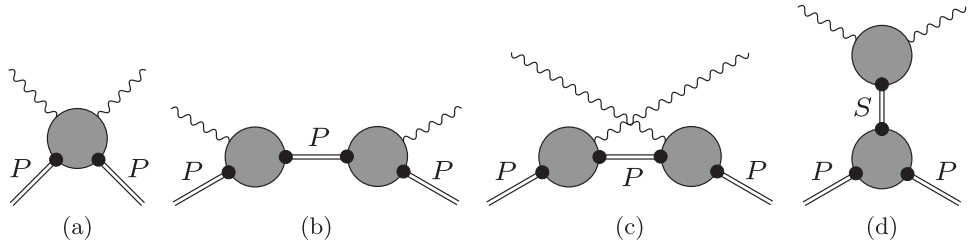

FIG. 2. Diagrams (a)–(d) contributing to Compton scattering tensor $M_{\mu\nu}$. The gray circles denote all possible one-particle irreducible contributions.

$$A^{\mathrm{Born}}(\nu^2,t)=-\frac{e^2t}{(s-M_\pi^2)(u-M_\pi^2)},$$
$$B^{\mathrm{Born}}(\nu^2,t)=-\frac{8e^2}{(s-M_\pi^2)(u-M_\pi^2)}.$$

The electric α_{E} and magnetic β_{M} polarizabilities are related to A^{NB}, B^{NB} by means of the following equations (see Refs. [47,48]):

$$\alpha_{\mathrm{E}}+\beta_{\mathrm{M}}=-\frac{M}{8\pi}B^{\mathrm{NB}}(0,0), \tag{18}$$

$$\alpha_{\mathrm{E}}-\beta_{\mathrm{M}}=-\frac{1}{8\pi M}(2A^{\mathrm{NB}}(0,0)+M^2B^{\mathrm{NB}}(0,0)). \tag{19}$$

The diagrams that contribute to Compton tensor are shown in Fig. 2. Consider contribution of the diagrams shown in Figs. 2(a)–2(c) that form a gauge-invariant combination. The diagrams shown in Figs. 2(b), 2(c) contain kinematic singularities that are canceled by corresponding Born terms in Eq. (16). One can notice that, among these diagrams, only the diagram in Fig. 2(a) contains tensors proportional to $g_{\alpha\beta}$ and can be parametrized as

$$M^{(\mathrm{a})}_{\alpha\beta}=\left(-\frac{t}{2}A(\nu^2,t)+\nu^2B(\nu^2,t)\right)g_{\alpha\beta}+\text{other tensor structures},$$
$$M^{(\mathrm{a})\mathrm{NB}}_{\alpha\beta}=\left(-\frac{t}{2}A(\nu^2,t)+\nu^2B(\nu^2,t)-2\right)g_{\alpha\beta}+\text{other tensor structures}, \tag{20}$$

according to formulas (16) and (17). The amplitudes A, B that appear in definition of polarizabilities (18), (19) can be extracted from coefficient of $g_{\alpha\beta}$ in $M^{\mathrm{NB}}_{\alpha\beta}$ with the help of formulas

$$A^{\mathrm{NB}}(0,0)=-2\frac{\partial}{\partial t}\left(-\frac{t}{2}A(\nu^2,t)+\nu^2B(\nu^2,t)-2\right)\Big|_{t=0,\nu=0},$$
$$B^{\mathrm{NB}}(0,0)=\frac{1}{2}\frac{\partial^2}{\partial^2\nu}\left(-\frac{t}{2}A(\nu^2,t)+\nu^2B(\nu^2,t)-2\right)\Big|_{t=0,\nu=0}.$$

It is therefore sufficient to calculate only the diagram in Fig. 2(a) of gauge-invariant combination of the diagrams in Figs. 2(a)–2(c) in order to extract electric and magnetic dipole polarizabilities. This is more straightforward because the diagram in Fig. 2(a) does not contain kinematic poles. One-loop contributions of this type are shown in Fig. 3 [the Feynman rules in Euclidean space are given by formulas (2), (6), and (7) for loops, Eqs. (10), (12), (13)

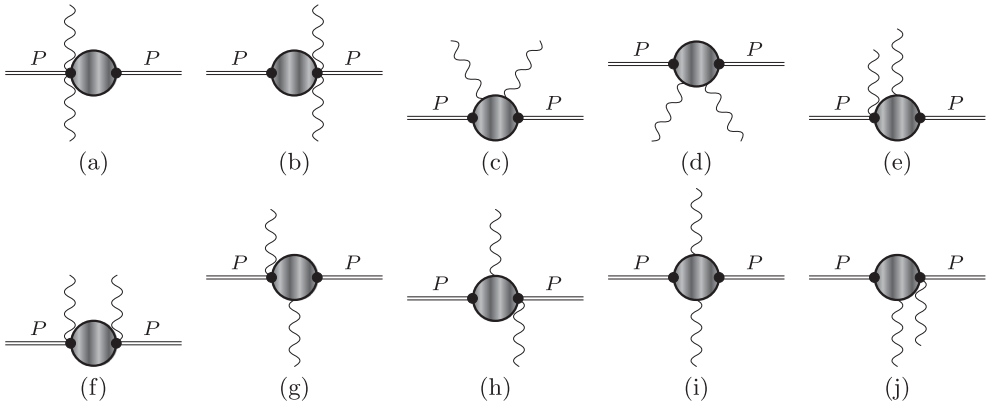

FIG. 3. The one-loop diagrams (a)–(j) contributing to $M^{(a)}_{\alpha\beta}$. Wavy filling represents the vacuum gluon field (9). The diagrams related by crossings are not shown.

describe nonlocal vertices that should be multiplied by corresponding h_Q, the local vertices are the same as in QED, and the quark propagators are defined by Eq. (11)]. For example, Fig. 3(e) corresponds to

$$(2\pi)^4\delta^{(4)}(p'+q'-p-q)M_{\mu\nu}^{(\mathrm{a,e})} = e^2h_P^2\int d\sigma_B\int d^4x\int d^4y\int d^4z\exp(ipx+iqx-ip'y-iq'z)$$
$$\times(-1)\mathrm{Tr}V_\mu^{aP00}(x;-q)S(x,y)V^{bP00}(y)S(y,z)Q\gamma_\nu S(z,y)$$
$$+\text{ crossed term},$$

for two external pseudoscalar ground-state mesons (see the Appendix for details).

The contribution to the amplitude corresponding to the diagram with intermediate scalar fields shown in Fig. 2(d) is separately gauge invariant and can be represented as

$$\varepsilon^\alpha(q)\varepsilon^{*\beta}(q')M_{\alpha\beta}^{(d)} = \varepsilon^\alpha(q)\varepsilon^{*\beta}(q')\sum_S\Gamma_{\alpha\beta}^{S\gamma\gamma}D_Sh_P^2\Gamma_{SPP}, \quad (21)$$

where $\Gamma_{S\gamma\gamma}$ parametrizes the $S\to\gamma\gamma$ subprocess, D_S is a scalar meson field propagator, $h_P^2\Gamma_{SPP}(t)$ describes the transition of the scalar field to a couple of pseudoscalar mesons (corresponding one-loop diagrams are shown in Fig. 4, the formulas are given in the Appendix). Diagram $M^{(d)}$ does not contain the tensor $T_{2\alpha\beta}$ [see formula (17)] and hence contributes only to amplitude A.

The computational complexity of the amplitudes that we need to evaluate in order to extract polarizabilities quickly grows with increasing the radial number n taken into account for the diagonalization of the quadratic part of the action. In the present paper, for numerical calculation only $n=0$ states are taken into account, such that the matrix $\mathcal{O}$ in Eq. (3) is reduced to the unity matrix, and the higher radial states are neglected. The values of parameters in this lowest approximation with respect to the "radial excitation mixing" are given in Table I (for detailed discussion see Ref. [35]).

The values of polarizabilities found in the present work are presented in Table II. Since no small-momentum expansion is employed, we can also calculate polarizabilities of kaons. In contrast with results obtained in several distinct quark-meson models [27,28,30], the main contribution in the model under consideration comes from one-loop diagrams, while the contribution of the intermediate scalar field is less important. However, this can be considered as a rearrangement of contributions because only their sum is observable.

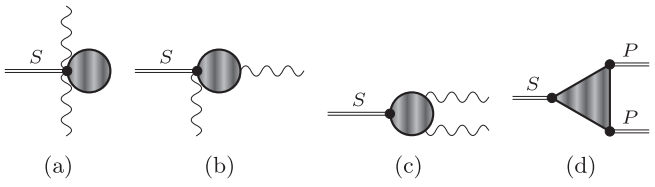

FIG. 4. One-loop diagrams contributing to $M_{\alpha\beta}^S$ in formula (21) (crossed diagrams are not shown). Diagrams (a),(b),(c) are related to $\Gamma_{S\gamma\gamma}$, diagram (d) results in $h_P^2\Gamma_{SPP}$.

IV. DISCUSSION

We investigated dipole polarizabilities of the light pseudoscalar mesons in the framework of the nonlocal effective meson action obtained within the mean-field approach to QCD vacuum. The model described by the functional (14) allows consistent treatment of various phenomena of low-energy hadronic physics: spectra of mesons, their decay constants, and form factors. Comparison of the present formalism with other approaches like functional renormalization group, Dyson-Schwinger equations, lattice QCD, and anti–de Sitter/QCD is outlined in [35].

The values of charged pion polarizabilities calculated in the present study are in agreement with COMPASS data and most recent two-loop ChPT calculation [7]. The pion mass and leptonic decay constant evaluated in the same framework earlier [35] agree with experimental data, and these values serve as phenomenological input for the basic Lagrangian of ChPT. The agreement with ChPT then follows from the identification of a pion as a pseudo-Goldstone boson of broken chiral symmetry. Moreover, an effective low-energy Lagrangian for pions can be obtained from generating functional (14) if one integrates out heavier fields and performs an expansion in small momenta of pions. It is clear that such an analysis would be technically complicated, and it deserves a separate investigation that would be interesting to perform, and we hope to do it in due course.

The prediction of lattice QCD for polarizabilities depends on parameters such as the lattice volume, lattice

TABLE I. Values of parameters used for calculations of polarizabilities that were extracted from the experimental values of masses of π, ρ, K, K^* via Eq. (5). The values of quark masses are largely affected by the presence of background gluon field, and they are not in exact one-to-one correspondence with the values of masses in models without background gluon field, see, e.g., Ref. [35].

$m_{u/d}$(MeV)	m_s(MeV)	Λ(MeV)	α_s
174.8	393.3	439.7	6.23

TABLE II. Numerical results for polarizabilities of pseudoscalar mesons in Gaussian units of 10^{-4} fm^3. Column "Diagrams in Fig. 3" corresponds to the leading-order contribution of the diagrams shown in Figs. 2(a)–2(c), which is extracted from diagrams in Fig. 3 with formula (20). "Diagrams in Fig. 4" labels the leading-order contribution of the diagrams with intermediate scalar quark-antiquark fields shown in Fig. 2(d), which is given by formula (21).

		Diagrams in Fig. 3	Diagrams in Fig. 4	Total	Experiment	ChPT
$\pi^{\pm}$	$\alpha_E+\beta_M$	0.13	0	0.13	$0.5\pm0.5_{\text{stat}}$ [4]	0.16 [7]
	$\alpha_E-\beta_M$	4.82	1.48	6.3	$4.0\pm1.2_{\text{stat}}\pm1.4_{\text{syst}}$ [4]	5.7 [7]
π^0	$\alpha_E+\beta_M$	0.71	0	0.71	0.98 ± 0.03 [32]	1.15 [11]
	$\alpha_E-\beta_M$	−0.26	1.48	1.22	-1.6 ± 2.2 [32]	−1.9 [11]
$K^{\pm}$	$\alpha_E+\beta_M$	0.41	0	0.41		
	$\alpha_E-\beta_M$	1.22	0.47	1.69		
$K^0,\bar{K}^0$	$\alpha_E+\beta_M$	0.62	0	0.62		
	$\alpha_E-\beta_M$	−0.29	0.17	−0.12		

spacings, and quark masses. The value of dipole magnetic polarizability of charged pion found in paper [16] with the finest lattice is $\beta_{\pi^{\pm}}=-2.06\pm0.76\times10^{-4}$ fm^3, which supports the data of the COMPASS collaboration [4], ChPT [7], and the findings of this paper.

The distinctive feature of the present approach is that mesons are extended collective excitations of quark-antiquark and gluon fields in the confining gluon background field. The structure of meson is encoded in the nonlocal meson-quark vertices (10), which are straightforwardly calculated. The nonlocality of meson-quark vertices leads to meson-quark-photon interactions given by Eqs. (12), (13). Another feature of the present approach is that the intermediate scalar quark-antiquark field cannot be identified with physical light scalar meson because corresponding propagator has no pole at real momenta. Even though there are no light scalar quark-antiquark particles, the corresponding field contributes to dipole polarizabilities. As a result of these features, the contributions to polarizabilities are arranged differently from other quark-meson models [27,28,30], and the main contribution to polarizabilities in the model under consideration comes from one-loop diagrams in Fig. 3.

Besides ground-state scalar fields, the effective meson action (14) contains other scalar fields. For instance, it includes the scalar component of orbitally excited vector meson field emerging from hyperfine splitting, with meson-quark vertices given by

$$V^{a01n}_{\mu\mu}=\frac{1}{4}\mathcal{C}_{1n}\mathcal{M}^a\gamma^\mu F_{n1}\left(\frac{\overleftrightarrow{\mathcal{D}}^2(x)}{\Lambda^2}\right)\frac{1}{i}\frac{\overleftrightarrow{\mathcal{D}}_\mu(x)}{\Lambda}.$$

The inverse propagator of a corresponding isosinglet field in ground radial state $n=0$ at real momenta is shown in Fig. 5. One expects that the contribution to dipole polarizabilities of these fields via diagram in Fig. 2(d) is smaller than the contribution of a ground-state scalar quark-antiquark field (the inverse propagator is shown in Fig. 1) if for no other reason than their propagator is also smaller at $p^2=0$. A thorough investigation of this contribution, however, is even more complex than the contribution of ground-state scalar quark-antiquark field. The zero of the inverse propagator shown in Fig. 5 is located at $\sqrt{p^2}=1252-i203$ MeV. In contrast, it was found that the inverse propagator of the ground-state scalar quark-antiquark field has no zeroes in the complex plane in a physically relevant region $|p^2|<(2\text{ GeV})^2$.

The computation has been performed in the lowest approximation with respect to the mixing of radially excited states in the functional (14), and it would be interesting and important to check the stability of obtained results in this respect by accounting the higher radial excitations, which will also allow one to estimate the polarizabilities of radially excited pion and kaon states. However, the latter has mostly purely theoretical importance as an experimental measurement seems to be hardly achievable. More detailed discussion about the relation of the present approach to ChPT is an interesting issue that we expect to address in future work.

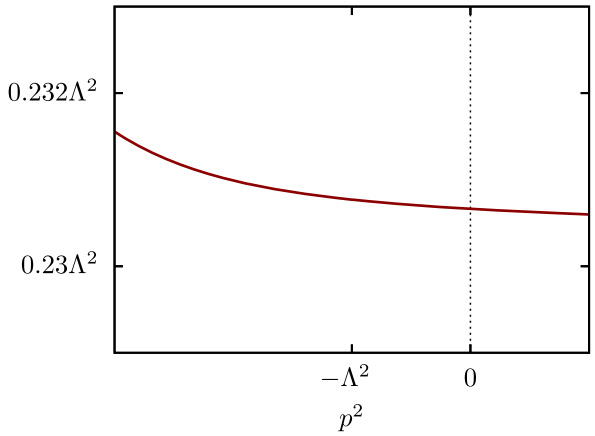

FIG. 5. The inverse propagator for scalar field emerging from hyperfine splitting of orbital excitation of vector meson field with respect to Euclidean momenta p^2.

ACKNOWLEDGMENTS

We are grateful for resources provided by "Govorun" supercomputer at the Joint Institute for Nuclear Research.

APPENDIX: EVALUATION OF DIAGRAMS

1. Formulas for diagrams in Fig. 3

The notations are given in Secs. II and III. Indices a, b correspond to combination of flavor matrices for a given pseudoscalar ground-state meson. The one-loop contribution to $M^{(a)}_{\mu\nu}$ in Fig. 2 is given by

$$M^{(\mathrm{a})}_{\mu\nu} = \sum_{\mathrm{k=a,b,c,d,e,f,g,h,i,j}} M^{(\mathrm{a,k})}_{\mu\nu} + \text{crossed diagrams}.$$

Here $M^{(\mathrm{a,k})}_{\mu\nu}$ are given by diagrams in Fig. 3:

$$(2\pi)^4\delta^{(4)}(p'+q'-p-q)M^{(\mathrm{a,a})}_{\mu\nu} = e^2h_P^2\int d\sigma_B\int d^4x\int d^4y\exp(ipx+iqx-iq'x-ip'y) \times(-1)\mathrm{Tr}V^{aP00}_{\mu\nu}(x;-q,q')S(x,y)V^{bP00}(y)S(y,x), \tag{A1}$$

$$(2\pi)^4\delta^{(4)}(p'+q'-p-q)M^{(\mathrm{a,b})}_{\mu\nu} = e^2h_P^2\int d\sigma_B\int d^4x\int d^4y\exp(ipx+iqy-iq'y-ip'y) \times(-1)\mathrm{Tr}V^{aP00}(x)S(x,y)V^{bP00}_{\mu\nu}(y;-q,q')S(y,x), \tag{A2}$$

$$(2\pi)^4\delta^{(4)}(p'+q'-p-q)M^{(\mathrm{a,c})}_{\mu\nu} = e^2h_P^2\int d\sigma_B\int d^4x\int d^4y\int d^4z_1\int d^4z_2\exp(ipx-ip'y+iqz_1-iq'z_2) \times(-1)\mathrm{Tr}V^{aP00}(x)S(x,y)V^{bP00}(y)S(y,z_1)Q\gamma_\mu S(z_1,z_2)Q\gamma_\nu S(z_2,x), \tag{A3}$$

$$(2\pi)^4\delta^{(4)}(p'+q'-p-q)M^{(\mathrm{a,d})}_{\mu\nu} = e^2h_P^2\int d\sigma_B\int d^4x\int d^4y\int d^4z_1\int d^4z_2\exp(ipx-ip'y+iqz_1-iq'z_2) \times(-1)\mathrm{Tr}V^{aP00}(x)S(x,z_1)Q\gamma_\mu S(z_1,z_2)Q\gamma_\nu S(z_2,y)V^{bP00}(y)S(y,x), \tag{A4}$$

$$(2\pi)^4\delta^{(4)}(p'+q'-p-q)M^{(\mathrm{a,e})}_{\mu\nu} = e^2h_P^2\int d\sigma_B\int d^4x\int d^4y\int d^4z\exp(ipx+iqx-ip'y-iq'z) \times(-1)\mathrm{Tr}V^{aP00}_{\mu}(x;-q)S(x,y)V^{bP00}(y)S(y,z)Q\gamma_\nu S(z,y), \tag{A5}$$

$$(2\pi)^4\delta^{(4)}(p'+q'-p-q)M^{(\mathrm{a,f})}_{\mu\nu} = e^2h_P^2\int d\sigma_B\int d^4x\int d^4y\int d^4z\exp(ipx+iqx-ip'y-iq'y) \times(-1)\mathrm{Tr}V^{aP00}_{\mu}(x;-q)S(x,y)V^{bP00}_{\nu}(y;q')S(y,x), \tag{A6}$$

$$(2\pi)^4\delta^{(4)}(p'+q'-p-q)M^{(\mathrm{a,g})}_{\mu\nu} = e^2h_P^2\int d\sigma_B\int d^4x\int d^4y\int d^4z\exp(ipx+iqx-iq'z-ip'y) \times(-1)\mathrm{Tr}V^{aP00}_{\mu}(x;-q)S(x,z)Q\gamma_\nu S(z,y)V^{bP00}(y)S(y,x), \tag{A7}$$

$$(2\pi)^4\delta^{(4)}(p'+q'-p-q)M^{(\mathrm{a,h})}_{\mu\nu} = e^2h_P^2\int d\sigma_B\int d^4x\int d^4y\int d^4z\exp(ipx+iqy-ip'y-iq'z) \times(-1)\mathrm{Tr}V^{aP00}(x)S(x,y)V^{bP00}_{\mu}(y;-q)S(y,z)Q\gamma_\nu S(z,x), \tag{A8}$$

$$(2\pi)^4\delta^{(4)}(p'+q'-p-q)M^{(\mathrm{a,i})}_{\mu\nu} = e^2h_P^2\int d\sigma_B\int d^4x\int d^4y\int d^4z_1\int d^4z_2\exp(ipx-ip'y+iqz_1-iq'z_2) \times(-1)\mathrm{Tr}V^{aP00}(x)S(x,z_1)Q\gamma_\mu S(z_1,y)V^{bP00}(y)S(y,z_2)Q\gamma_\nu S(z_2,x), \tag{A9}$$

$$(2\pi)^4\delta^{(4)}(p'+q'-p-q)M^{(\mathrm{a,j})}_{\mu\nu} = e^2h_P^2\int d\sigma_B\int d^4x\int d^4y\int d^4z\exp(ipx+iqz-ip'y-iq'y) \times(-1)\mathrm{Tr}V^{aP00}(x)S(x,z)Q\gamma_\mu S(z,y)V^{bP00}_{\mu}(y;q')S(y,x). \tag{A10}$$

The trace is taken with respect to flavor, color, and spinor indices. Crossed diagrams can be obtained by $q \leftrightarrow q', \mu \leftrightarrow \nu$. The vertex operator

$$V^{aP00}(x) = \mathcal{M}^a i\gamma_5 \int_0^1 dt \, \exp\left(\frac{\overleftrightarrow{\mathcal{D}}^2(x)}{\Lambda^2} t\right)$$

is a function of $\overleftrightarrow{\mathcal{D}}_\mu$, which acts as

$$\begin{aligned} S_f(y-x)\overleftrightarrow{\mathcal{D}}_\mu(x) S_{f'}(x-z) &= e^{-\frac{i}{2}y_\mu \hat{B}_{\mu\nu} x_\nu} \int \frac{d^4p}{(2\pi)^4} e^{-ip(y-x)} \tilde{H}_f(p) \overleftrightarrow{\mathcal{D}}_\mu(x) e^{-\frac{i}{2}x_\mu \hat{B}_{\mu\nu} z_\nu} \int \frac{d^4q}{(2\pi)^4} e^{-iq(x-z)} \tilde{H}_{f'}(q), \\ &= \int \frac{d^4p}{(2\pi)^4} \int \frac{d^4q}{(2\pi)^4} e^{-\frac{i}{2}y_\mu \hat{B}_{\mu\nu} x_\nu} e^{-ip(y-x)} \tilde{H}_f(p) \left\{ \xi_f \left[ip_\mu - \frac{i}{2}\hat{B}_{\mu\nu}(x_\nu - y_\nu) \right] \right. \\ &\quad \left. + \xi_{f'} \left[iq_\mu - \frac{i}{2}\hat{B}_{\mu\nu}(x_\nu - z_\nu) \right] \right\} \times e^{-\frac{i}{2}x_\mu \hat{B}_{\mu\nu} z_\nu} e^{-iq(x-z)} \tilde{H}_{f'}(q). \end{aligned}$$

The loop integrals are finite due to nonlocal meson vertices, so no regularization is needed. With meson vertices and quark propagators given by formulas (10) and (11), the space and momentum integrals are Gaussian and can be computed analytically. The averaging over the background field is performed with the help of formula (8) where tensor $J_{\mu\nu}$ is a combination of external momenta of mesons and photons.

After these straightforward transformations one arrives at integrals over proper times s_i, t_i that originate from vertices and propagators. These integrals are computed numerically. Unfortunately, the analytical expressions are too cumbersome to be presented here.

2. Formulas for diagrams in Fig. 4

The one-loop contribution to $\Gamma^{S\gamma\gamma}_{\mu\nu}$ is given by

$$\Gamma^{S\gamma\gamma}_{\mu\nu} = \Gamma^{(a)S\gamma\gamma}_{\mu\nu} + \Gamma^{(b)S\gamma\gamma}_{\mu\nu} + \Gamma^{(c)S\gamma\gamma}_{\mu\nu} + \text{crossed diagrams},$$

where $\Gamma^{(k)S\gamma\gamma}_{\mu\nu}$ are given by the diagrams in Figs. 4(a)–4(c). The one-loop contribution to Γ^{SPP} is given by the diagrams in Fig. 4(d):

$$(2\pi)^4\delta^{(4)}(p'+q'-p-q)\Gamma^{(a)S\gamma\gamma}_{\mu\nu} = e^2 \int d\sigma_B \int d^4x \, \exp(ipx - ip'x + iqx - iq'x)(-1)\mathrm{Tr} V^{aS00}_{\mu\nu}(x;-q,q')S(x,x), \quad \text{(A11)}$$

$$\begin{aligned} (2\pi)^4\delta^{(4)}(p'+q'-p-q)\Gamma^{(b)S\gamma\gamma}_{\mu\nu} &= e^2 \int d\sigma_B \int d^4x \int d^4z \, \exp(ipx - ip'x + iqx - iq'z) \\ &\quad \times (-1)\mathrm{Tr} V^{aS00}_{\mu}(x;-q)S(x,z)Q\gamma_\nu S(z,x), \end{aligned} \quad \text{(A12)}$$

$$\begin{aligned} (2\pi)^4\delta^{(4)}(p'+q'-p-q)\Gamma^{(c)S\gamma\gamma}_{\mu\nu} &= e^2 \int d\sigma_B \int d^4x \int d^4z_1 \int d^4z_2 \, \exp(ipx - ip'x + iqz_1 - iq'z_2) \\ &\quad \times (-1)\mathrm{Tr} V^{aS00}(x)S(x,z_1)Q\gamma_\mu S(z_1,z_2)Q\gamma_\nu S(z_2,y), \end{aligned} \quad \text{(A13)}$$

$$\begin{aligned} (2\pi)^4\delta^{(4)}(p'+q'-p-q)h_P^2\Gamma^{SPP} &= h_P^2 \int d\sigma_B \int d^4x \int d^4y \int d^4z \, \exp(iqx - iq'x - ip'y + ipz) \\ &\quad \times (-1)\mathrm{Tr} V^{aS00}(x)S(x,y)V^{bP00}(y)S(y,z)V^{cP00}(z)S(z,y). \end{aligned} \quad \text{(A14)}$$

The scalar two-point correlation function is an example where the final formula used for numerical computation has a concise form:

$$\Gamma^{(2)}_{abS}(x-y) = \int d\sigma_B \mathrm{Tr} V^{aS00}(x) S(x,y) V^{bS00}(y) S(y,x),$$

$$\tilde{\Gamma}^{(2)}_{abS}(p) = \mathrm{Tr}(\mathcal{M}^a\mathcal{M}^b)\frac{\Lambda^2}{4\pi^2}\mathrm{Tr}_v \int_0^1 dt_1 \int_0^1 dt_2 \int_0^1 ds_1 \int_0^1 ds_2 \left(\frac{1-s_1}{1+s_1}\right)^{m_f^2/4v\Lambda^2}\left(\frac{1-s_2}{1+s_2}\right)^{m_{f'}^2/4v\Lambda^2}$$
$$\times \frac{1}{\Phi_2^2}\left[\frac{p^2}{\Lambda^2}\frac{F_1}{\Phi_2^2} + \frac{m_f m_{f'}}{\Lambda^2}\frac{F_2}{(1-s_1^2)(1-s_2^2)} + \frac{F_3}{\Phi_2}\right]\exp\left\{-\frac{p^2}{2v\Lambda^2}\frac{\Phi_1}{\Phi_2}\right\},$$

where

$$\Phi_1 = s_1 s_2 + 2(\xi^2_{f'} s_1 + \xi^2_f s_2)(t_1+t_2)v,$$
$$\Phi_2 = s_1 + s_2 + 2(1+s_1 s_2)(t_1+t_2)v + 16(\xi^2_{f'} s_1 + \xi^2_f s_2) t_1 t_2 v^2,$$
$$F_1 = (1+s_1 s_2)[2(\xi_{f'} s_1 + \xi_f s_2)(t_1+t_2)v + 4\xi_f\xi_{f'}(1+s_1 s_2)(t_1+t_2)^2 v^2 + s_1 s_2(1-16\xi_f\xi_{f'} t_1 t_2 v^2)],$$
$$F_2 = (1+s_1 s_2)^2,$$
$$F_3 = 4v(1+s_1 s_2)(-1+16\xi_f\xi_{f'} t_1 t_2 v^2).$$

Analogous formulas for $\Gamma_{V,P}$ obtained in Ref. [35] describe the spectrum of radially excited mesons: light, heavy-light mesons, and heavy quarkonia.

[1] M. A. Ivanov, Pion polarizabilities: Theory vs experiment, Int. J. Mod. Phys. Conf. Ser. **39**, 1560104 (2015).
[2] M. Moinester and S. Scherer, Compton scattering off pions and electromagnetic polarizabilities, Int. J. Mod. Phys. A **34**, 1930008 (2019).
[3] M. Moinester, Pion polarizability 2022 status report, arXiv:2205.09954.
[4] C. Adolph *et al.* (COMPASS Collaboration), Measurement of the Charged-Pion Polarizability, Phys. Rev. Lett. **114**, 062002 (2015).
[5] J. Bijnens and F. Cornet, Two pion production in photon-photon collisions, Nucl. Phys. **B296**, 557 (1988).
[6] M. V. Terentev, Pion polarizability, virtual compton-effect and $\pi \to e\nu\gamma$ decay, Yad. Fiz. **16**, 162 (1972) [Sov. J. Nucl. Phys. **16**, 87 (1973)].
[7] J. Gasser, M. A. Ivanov, and M. E. Sainio, Revisiting $\gamma\gamma \to \pi^+\pi^-$ at low energies, Nucl. Phys. **B745**, 84 (2006).
[8] U. Burgi, Charged pion pair production and pion polarizabilities to two loops, Nucl. Phys. **B479**, 392 (1996).
[9] U. Burgi, Charged pion polarizabilities to two loops, Phys. Lett. B **377**, 147 (1996).
[10] S. Bellucci, J. Gasser, and M. E. Sainio, Low-energy photon-photon collisions to two loop order, Nucl. Phys. **B423**, 80 (1994); **B431**, 413(E) (1994).
[11] J. Gasser, M. A. Ivanov, and M. E. Sainio, Low-energy photon-photon collisions to two loops revisited, Nucl. Phys. **B728**, 31 (2005).
[12] H. R. Fiebig, W. Wilcox, and R. M. Woloshyn, A study of hadron electric polarizability in quenched lattice QCD, Nucl. Phys. **B324**, 47 (1989).
[13] F. X. Lee, L. Zhou, W. Wilcox, and J. C. Christensen, Magnetic polarizability of hadrons from lattice QCD in the background field method, Phys. Rev. D **73**, 034503 (2006).
[14] M. Lujan, A. Alexandru, W. Freeman, and F. Lee, Electric polarizability of neutral hadrons from dynamical lattice QCD ensembles, Phys. Rev. D **89**, 074506 (2014).
[15] W. Freeman, A. Alexandru, M. Lujan, and F. X. Lee, Sea quark contributions to the electric polarizability of hadrons, Phys. Rev. D **90**, 054507 (2014).
[16] E. V. Luschevskaya, O. E. Solovjeva, and O. V. Teryaev, Magnetic polarizability of pion, Phys. Lett. B **761**, 393 (2016).
[17] M. Lujan, A. Alexandru, W. Freeman, and F. X. Lee, Finite volume effects on the electric polarizability of neutral hadrons in lattice QCD, Phys. Rev. D **94**, 074506 (2016).
[18] G. S. Bali, B. B. Brandt, G. Endrődi, and B. Gläßle, Meson masses in electromagnetic fields with Wilson fermions, Phys. Rev. D **97**, 034505 (2018).
[19] H. Niyazi, A. Alexandru, F. X. Lee, and M. Lujan, Charged pion electric polarizability from lattice QCD, Phys. Rev. D **104**, 014510 (2021).
[20] R. Bignell, W. Kamleh, and D. Leinweber, Pion magnetic polarisability using the background field method, Phys. Lett. B **811**, 135853 (2020).
[21] H. T. Ding, S. T. Li, A. Tomiya, X. D. Wang, and Y. Zhang, Chiral properties of $(2+1)$-flavor QCD in strong magnetic fields at zero temperature, Phys. Rev. D **104**, 014505 (2021).

[22] W. Wilcox and F. X. Lee, Towards charged hadron polarizabilities from four-point functions in lattice QCD, Phys. Rev. D **104**, 034506 (2021).
[23] A. I. L'vov, Pion polarizabilities in the sigma model with quarks, Sov. J. Nucl. Phys. **34**, 289 (1981).
[24] M. K. Volkov and D. Ebert, Pion polarizability in a chiral quark model, Phys. Lett. B **101**, 252 (1981).
[25] M. K. Volkov and A. A. Osipov, Polarizability of pions and kaons in superconductor quark model (in Russian), Yad. Fiz. **41**, 1027 (1985).
[26] V. Bernard, B. Hiller, and W. Weise, Pion electromagnetic polarizability and chiral models, Phys. Lett. B **205**, 16 (1988).
[27] M. A. Ivanov and T. Mizutani, Pion and kaon polarizabilities in the quark confinement model, Phys. Rev. D **45**, 1580 (1992).
[28] A. E. Dorokhov, M. K. Volkov, J. Hufner, S. P. Klevansky, and P. Rehberg, Pion polarizabilities at finite temperature, Z. Phys. C **75**, 127 (1997).
[29] J. F. Donoghue and B. R. Holstein, Photon-photon scattering, pion polarizability and chiral symmetry, Phys. Rev. D **48**, 137 (1993).
[30] B. Hiller, W. Broniowski, A. A. Osipov, and A. H. Blin, Quadrupole polarizabilities of the pion in the Nambu–Jona-Lasinio model, Phys. Lett. B **681**, 147 (2009).
[31] L. V. Filkov, I. Guiasu, and E. E. Radescu, Pion polarizabilities from backward and fixed-u sum rules, Phys. Rev. D **26**, 3146 (1982).
[32] L. V. Fil'kov and V. L. Kashevarov, Compton scattering on the charged pion and the process $\gamma\gamma \to \pi^0\pi^0$, Eur. Phys. J. A **5**, 285 (1999).
[33] L. V. Fil'kov and V. L. Kashevarov, Determination of $\pi^{\pm}$ meson polarizabilities from the $\gamma\gamma \to \pi^+\pi^-$ process, Phys. Rev. C **73**, 035210 (2006).
[34] A. C. Kalloniatis and S. N. Nedelko, Realization of chiral symmetry in the domain model of QCD, Phys. Rev. D **69**, 074029 (2004); **70**, 119903(E) (2004).
[35] S. N. Nedelko and V. E. Voronin, Regge spectra of excited mesons, harmonic confinement and QCD vacuum structure, Phys. Rev. D **93**, 094010 (2016).
[36] S. N. Nedelko and V. E. Voronin, Influence of confining gluon configurations on the $P \to \gamma^*\gamma$ transition form factors, Phys. Rev. D **95**, 074038 (2017).
[37] S. N. Nedelko and V. E. Voronin, Domain wall network as QCD vacuum and the chromomagnetic trap formation under extreme conditions, Eur. Phys. J. A **51**, 45 (2015).
[38] S. N. Nedelko and V. E. Voronin, Energy-driven disorder in mean field QCD, Phys. Rev. D **103**, 114021 (2021).
[39] G. V. Efimov and S. N. Nedelko, Nambu–Jona-Lasinio model with the homogeneous background gluon field, Phys. Rev. D **51**, 176 (1995).
[40] Ja. V. Burdanov, G. V. Efimov, S. N. Nedelko, and S. A. Solunin, Meson masses within the model of induced nonlocal quark currents, Phys. Rev. D **54**, 4483 (1996).
[41] J. R. Pelaez, From controversy to precision on the sigma meson: A review on the status of the non-ordinary $f_0(500)$ resonance, Phys. Rep. **658**, 1 (2016).
[42] J. Terning, Gauging nonlocal Lagrangians, Phys. Rev. D **44**, 887 (1991).
[43] S. Nedelko, A. Nikolskii, and V. Voronin, Soft gluon fields and anomalous magnetic moment of muon, J. Phys. G **49**, 035003 (2022).
[44] R. Tarrach, Invariant amplitudes for virtual compton scattering off polarized nucleons free from kinematical singularities, zeros and constraints, Nuovo Cimento A **28**, 409 (1975).
[45] W. A. Bardeen and W. K. Tung, Invariant amplitudes for photon processes, Phys. Rev. **173**, 1423 (1968); **4**, 3229(E) (1971).
[46] A. I. L'vov, S. Scherer, B. Pasquini, C. Unkmeir, and D. Drechsel, Generalized dipole polarizabilities and the spatial structure of hadrons, Phys. Rev. C **64**, 015203 (2001).
[47] I. Guiasu and E. E. Radescu, Higher multipole polarizabilities of hadrons from compton scattering amplitudes, Ann. Phys. (N.Y.) **120**, 145 (1979).
[48] I. Guiasu and E. E. Radescu, Higher multipole polarizabilities of hadrons from compton scattering amplitudes. II, Ann. Phys. (N.Y.) **122**, 436 (1979).